IOPscience iopscience.iop.org

Home Search Collections Journals About Contact us My IOPscience

Subpicosecond transient Raman scattering studies of field-induced electron transport in an $In_{0.53}Ga_{0.47}As$ based p–i–n nanostructure: direct observation of the effects of electron momentum randomization

This article has been downloaded from IOPscience. Please scroll down to see the full text article.

2006 J. Phys.: Condens. Matter 18 L585

(http://iopscience.iop.org/0953-8984/18/47/L01)

View the table of contents for this issue, or go to the journal homepage for more

Download details:
IP Address: 129.252.86.83
The article was downloaded on 28/05/2010 at 14:31

Please note that terms and conditions apply.

J. Phys.: Condens. Matter **18** (2006) L585–L592 doi:10.1088/0953-8984/18/47/L01

LETTER TO THE EDITOR

Subpicosecond transient Raman scattering studies of field-induced electron transport in an $In_{0.53}Ga_{0.47}As$ based p–i–n nanostructure: direct observation of the effects of electron momentum randomization

K T Tsen[1], Juliann G Kiang[2] and D K Ferry[3]

[1] Department of Physics and Astronomy, Arizona State University, Tempe, AZ 85287, USA
[2] Armed Forces Radiobiology Research Institute, Uniformed Services University of the Health Sciences, Bethesda, MD 20899, USA
[3] Department of Electrical Engineering, Arizona State University, Tempe, AZ 85287, USA

Received 28 September 2006, in final form 25 October 2006
Published 10 November 2006
Online at stacks.iop.org/JPhysCM/18/L585

Abstract
Subpicosecond transient Raman spectroscopy has been used to study electron transport properties of an $In_{0.53}Ga_{0.47}As$ based p–i–n nanostructure. Both the electron distribution function and the electron drift velocity have been directly measured as a function of the photoexcited electron–hole pair density. We have found that, at low electron–hole pair densities such as $n = 5 \times 10^{16}$ cm^{-3}, the electron distribution function has an extremely non-Maxwellian shape. However, as the photoexcited electron pair density gradually increases, the non-Maxwellian distribution gradually evolves into a shifted Maxwellian distribution. We attribute these findings to the direct effects of the role of electron–electron scattering in momentum randomization.

In recent years, the size of electronic devices has decreased to where typical critical dimensions are of the order of a few tens of nanometres. This size, when coupled with a typical device operation voltage (which is of the order of 1 V), suggests that carrier transient effects will be the dominant transport properties for electrons or holes in semiconductor nanostructures. There are two transient transport properties that are of particular interest: ballistic transport and velocity overshoot phenomena. The former corresponds to a transport phenomenon in which electrons travel with minimal scattering; the latter represents a transport phenomenon where the electron drift velocity is substantially greater than its steady state value. These two transport phenomena have generated tremendous interest due to their potential for greatly enhancing the performance of semiconductor devices [1–5].

Many theoretical (mainly, Monte Carlo simulations) and experimental efforts [6–16] have been made to investigate these interesting yet challenging transient carrier transport phenomena of semiconductors. The potential of using Raman spectroscopy to probe the properties of

carriers in semiconductors was first experimentally demonstrated by Mooradian in n-type GaAs [17]. Later, Wolff [18] developed a light scattering theory based upon a two-band model, including the effects of non-parabolicity of the conduction band. Hamilton and McWhorter [19] then developed a comprehensive theory for light scattering by carriers in semiconductors by taking into account the band structure effects. Jha *et al* [20] extended the Raman theory to include the quantum corrections arising from probing with ultrashort laser pulses as well as the inevitable non-equilibrium conditions encountered in an ultrashort pulse pump–probe experiment. Chia *et al* [21–23] presented a comprehensive theory of light scattering by electrons in semiconductors by taking into account the band structure effects, the effects of various electron scattering processes, the effects of probing with an ultrafast laser pulse, and the non-equilibrium conditions.

From all of the above discussions, it is known that single-particle scattering (SPS) associated with spin-density fluctuations provides a *direct* probe of the electron distribution function in semiconductors. Raman spectroscopy is, therefore, very well suited for studying electron transport under the application of an electric field. The first attempt in this direction was made by Mooradian and McWhorter [24]. They used a Q-switched Nd-YAlG laser with a pulse width of the order of 1 ns, synchronized with a pulsed electric field, to investigate electron distributions in n-GaAs for electric fields up to 2 kV cm^{-1}. They tried to describe the observed non-equilibrium electron distributions with a drifted Maxwellian distribution function. We note that electron velocity overshoot phenomenon was not observed by these authors partly because of insufficient electric field intensities and partly because of a relatively wide laser pulse width used in their experiments. Ralph and Wolga [25] used a cw Kr-ion pumped dye laser to study non-equilibrium carrier distributions in an electrically biased n^+–n^-–n^+ GaAs device. Here, the laser was chosen to operate near but below the bandgap of GaAs. They found that drifted Maxwellian distributions fitted their difference spectra provided that the effects of resonance enhancement in the Raman scattering cross section were considered. In these Raman experiments, carriers were either extrinsically doped or electrically injected into the GaAs samples. Recently, Grann *et al* [26–30] have investigated non-equilibrium electron distributions, electron drift velocities and non-equilibrium longitudinal optical (LO) phonon populations in a GaAs based p–i–n nanostructure by using picosecond/subpicosecond transient/time-resolved Raman spectroscopy. These authors have directly confirmed the existence of electron velocity overshoot phenomenon in semiconductors. We notice that although many-body effects play an important role in the electron transport properties, it is extremely difficult to directly observe these effects in semiconductors. Here, we have used transient subpicosecond Raman spectroscopy to study electron transport properties of an $In_{0.53}Ga_{0.47}As$ based p–i–n nanostructure under the application of an electric field. In particular, we have directly measured the electron distribution function and the electron drift velocity as a function of the photoexcited electron–hole pair density. Our experimental results provide a direct demonstration of the effects of electron momentum randomization in semiconductors, in that strongly non-Maxwellian distribution functions are observed to evolve into shifted Maxwellians as the carrier density is increased.

The $In_{0.53}Ga_{0.47}As$ based nanostructure used in this work consisted of an InP–$In_{0.53}Ga_{0.47}As$–InP p–i–n structure grown by molecular beam epitaxy on a (001)-oriented InP substrate. As shown in figure 1, the p-type region is composed of a 10 nm thick Zn-doped ($\cong 5 \times 10^{17}$ cm^{-3}) InP layer. The i-region is a 1 μm thick intrinsic $In_{0.53}Ga_{0.47}As$ layer. This is the active region probed by our Raman scattering experiments. The n-type region is made up of a 100 nm thick Si-doped ($\cong 5 \times 10^{17}$ cm^{-3}) InP layer. Gold contacts are established on both the p and n sides of the mesa-like p–i–n diode structure in order to apply an electric field. An opening of $\cong 0.25$ mm^2 in area is created in the gold layer on the p side of the diode so that

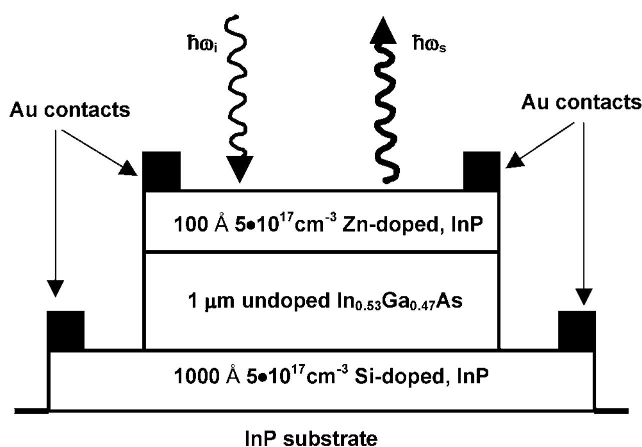

Figure 1. The $In_{0.53}Ga_{0.47}As$ based p–i–n nanostructure used in our transient subpicosecond Raman scattering experiments. Here, $\hbar\omega_i$, $\hbar\omega_s$ represent the photon energies of incident, scattered laser light, respectively.

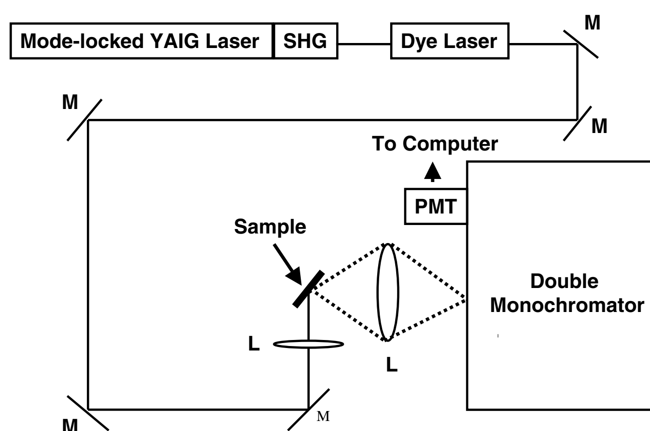

Figure 2. The experimental set-up for transient subpicosecond Raman spectroscopy. SHG: second-harmonic generation system; M: mirror; L: lens; PMT: photomultiplier tube.

light scattering experiments can be carried out. The Zn-doped p-type layer and Si-doped n-type layer together serve as a capacitor and provide a uniform electric field across the active region of the sample.

Figure 2 shows the experimental set-up for our subpicosecond Raman experiments. The output of the second harmonic of a cw mode-locked YAlG laser is used to synchronously pump a DCM dye laser. The dye laser, which has a pulse width of FWHM $=$ 800 fs, is chosen to operate at a photon energy of $\hbar\omega_L = 1.92$ eV with a repetition rate of 76 MHz. Since the same pulse is used for both excitation and probing of the non-equilibrium electron distribution, our results represent an average over the duration of the pulse width. The photoexcited electron–hole pair density was estimated from the average laser power, the focused spot size on the sample surface, and the absorption depth at the excitation laser wavelength. The backscattered Raman signals were collected and analysed by a standard computer-controlled Raman system, which includes a double spectrometer, a photomultiplier tube, and associated photon counting

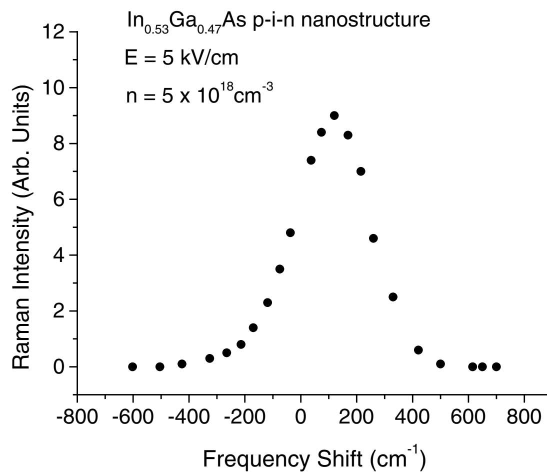

Figure 3. A typical SPS spectrum taken for an $In_{0.53}Ga_{0.47}As$ based p–i–n nanostructure, with an injected electron–hole pair density of $n = 5 \times 10^{18}$ cm^{-3} and an electric field intensity of $E = 5$ kV cm^{-1}.

electronics. All the data were taken at $T = 300$ K. The single-particle scattering (SPS) experiments, which were used to measure directly the electron distributions, were conducted in the $Z(X, Y)\bar{Z}$ scattering geometry; where $X = (100)$, $Y = (010)$ and $Z = (001)$. This scattering configuration ensures the detection of a scattered light signal from only spin-density fluctuations (SDF) [23, 24]. The effective electric field intensity during laser irradiation was determined from the Franz–Keldysh effect, as demonstrated in [31]. One important advantage of probing non-equilibrium excitations with Raman spectroscopy in semiconductors is that, since it detects a Raman signal only when excitation photons are present, the time resolution is essentially limited by the pulse width of the excitation laser and not by the response of the detection system. This explains why our detection system has a time resolution of the order of a nanosecond, whereas the time resolution in our Raman experiments is typically on the scale of subpicosecond. Another intriguing feature for probing carrier distributions with Raman spectroscopy is that, since the Raman scattering cross section is inversely proportional to the square of the effective mass of the carriers, it preferentially probes the electron distribution even if holes are simultaneously present. This unique feature makes the interpretation of the electron distribution in Raman scattering experiments much simpler than those from other techniques.

Figure 3 shows a typical SPS spectrum for an $In_{0.53}Ga_{0.47}As$ p–i–n nanostructure, taken at an injected electron–hole pair density of $n \cong 5 \times 10^{18}$ cm^{-3} and with electric field intensity $E = 5$ kV cm^{-1}. The SPS spectrum can be easily converted to the electron distribution function along the direction of the wavevector transfer of the photon as follows.

We first use conservation of both energy and momentum in the photon–electron scattering process and the energy-dependent electron effective mass derived from the $\vec{k} \cdot \vec{p}$ perturbation method [32–34] to convert frequency shift ω into corresponding electron velocity. The electron distribution function along the wavevector transfer direction is then obtained by multiplying the measured SPS cross section by the square of velocity-dependent effective mass to take into account the effect of non-parabolicity in the conduction band. The latter correction is necessary because the SPS cross section is inversely proportional to the square of the electron effective mass [17, 19, 23, 24]. The resultant electron distribution function obtained in such a way from the SPS spectrum of figure 3 is shown in figure 4(e).

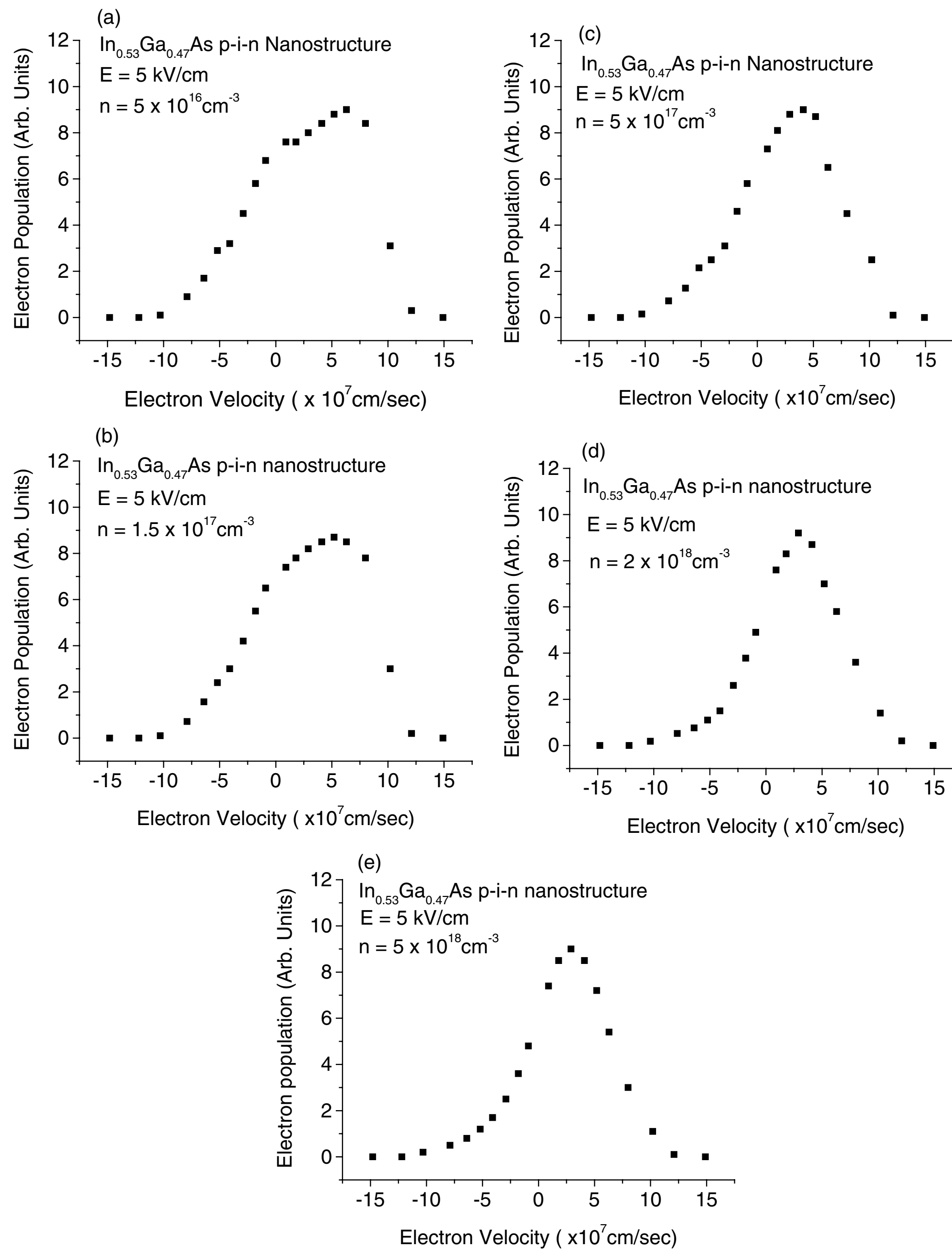

Figure 4. Typical non-equilibrium electron distributions for an $In_{0.53}Ga_{0.47}As$ based p–i–n nanostructure, taken at $E = 5$ kV cm^{-1}, and with (a) $n = 5 \times 10^{16}$ cm^{-3}, (b) $n = 1.5 \times 10^{17}$ cm^{-3}, (c) $n = 5 \times 10^{17}$ cm^{-3}, (d) $n = 2 \times 10^{18}$ cm^{-3} and (e) $n = 5 \times 10^{18}$ cm^{-3}. The electron distribution evolves from an extremely non-Maxwellian one to a shifted Maxwellian distribution as the photoexcited electron–hole pair density increases.

Figure 4(a) shows a typical non-equilibrium electron distribution for an $In_{0.53}Ga_{0.47}As$ based nanostructure, taken at an electric field intensity of $E = 5$ kV and for an electron–hole pair density of $n \cong 5 \times 10^{16}$ cm^{-3}. We notice that the electron distribution at such a low injected

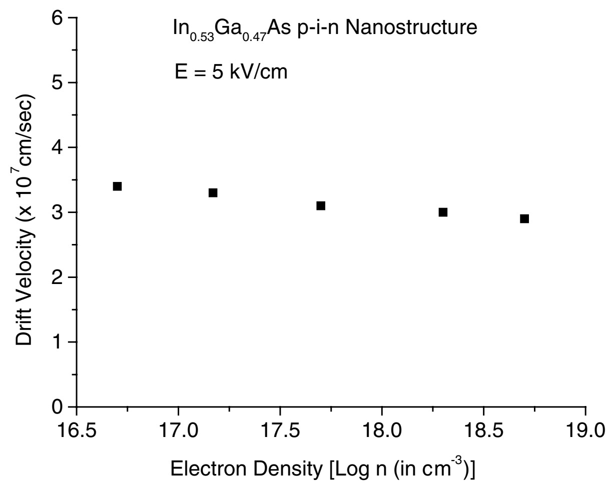

Figure 5. The electron drift velocity as a function of photoexcited electron–hole pair density for an $In_{0.53}Ga_{0.47}As$ based p–i–n nanostructure, taken at $E = 5$ kV cm^{-1}. Electron drift velocity decreases slightly as the photoexcited electron–hole pair density increases by two orders of magnitude.

electron–hole pair density exhibits an extremely non-equilibrium nature in that it can be fitted neither with a shifted Fermi–Dirac distribution nor with a shifted Maxwellian distribution. In addition, the sharp cut-off in the electron velocity around 1×10^8 cm s^{-1} is primarily due to electron intervalley scattering processes as well as the effect of band structure in $In_{0.53}Ga_{0.47}As$. However, as we increase the photoexcited electron–hole pair density, a dramatic change of the shape of electron distribution was observed. Figures 4(b)–(e) show non-equilibrium electron distributions for an $In_{0.53}Ga_{0.47}As$ based nanostructure, taken at an electric field intensity of $E = 5$ kV and with an injected electron–hole pair density of $n = 1.5 \times 10^{17}$, 5×10^{17}, 2×10^{18} and 5×10^{18} cm^{-3}, respectively. We note that when the injected electron–hole pair density increases from 5×10^{16} to 5×10^{18} cm^{-3}, the electron distribution evolves from an extremely asymmetric (non-Maxwellian) form to a shifted Maxwellian one. This is a manifestation of the effect of efficient electron–electron scattering processes at high electron–hole densities and provides a direct evidence of the effects of momentum randomization in semiconductors. The electron drift velocities have been found to be $V_d \cong (3.4 \pm 0.3) \times 10^7$, $(3.2 \pm 0.3) \times 10^7$, $(3.1 \pm 0.3) \times 10^7$, $(3.0 \pm 0.3) \times 10^7$ and $(2.9 \pm 0.3) \times 10^7$ cm s^{-1} for the five densities in figure 4 (from the lowest to the highest). As shown in figure 5, we observe that the electron drift velocity decreases slightly as the photoexcited electron–hole pair density increases over two orders of magnitude. This decrease is probably a result of the effect of the carrier density on the electron–LO phonon interaction as well as the direct electron–electron scattering itself.

In general, because of conservation of momentum, the effect of the electron–electron scattering process is not efficient in reducing the electron drift velocity. As a matter of fact, if we consider only two-particle interactions, then conservation of momentum predicts that there is no change of electron drift velocity as we vary the injected electron–hole pair density. However, the electrons also scatter off the collective excitations of the entire electron gas—an effect called electron–plasmon scattering [35–37]. As a result, the general role of electron–electron scattering will be to lower slightly the electron drift velocity and to drive the distribution function back toward a Maxwellian shape. This depletes the high energy tails that form particularly with polar mode scattering. All of these arguments are consistent with our experimental findings.

In conclusion, electron transport properties of an $In_{0.53}Ga_{0.47}As$ based p–i–n nanostructure have been studied by transient Raman spectroscopy on a subpicosecond timescale. Both the electron distribution function and the electron drift velocity have been directly measured as a function of the photoexcited electron–hole pair density. We have found that, at low electron–hole pair densities, the electron distribution function is extremely non-Maxwellian; as the photoexcited electron pair density slowly increases, the non-equilibrium electron distribution gradually evolves into a shifted Maxwellian distribution. We attribute these findings to the direct effects of electron–electron scattering on the momentum randomization in semiconductors.

This work is supported by the National Science Foundation under Grant No DMR-0305147.

References

[1] Ferry D K, Grubin H L and Iafrate G J 1984 *Semiconductors Probed by Ultrafast Laser Spectroscopy* vol 1, ed R R Alfano (New York: Academic) p 413
[2] Constant E 1985 *Hot Electron Transport in Semiconductors* (*Springer Topics in Applied Physics* vol 58) ed L Reggiani (Berlin: Springer) p 227
[3] Shah J and Leheny R F 1984 *Semiconductors Probed by Ultrafast Laser Spectroscopy* vol 1, ed R R Alfano (New York: Academic) p 45
[4] Tsen K T 2001 *Ultrafast Phenomena in Semiconductors* ed K T Tsen (New York: Springer) p 191
[5] Tsen K T 2004 *Ultrafast Dynamical Processes in Semiconductors* (*Springer Topics in Applied Physics* vol 92) ed K T Tsen (Heidelberg: Springer) p 193
[6] Ruch J G 1972 *IEEE Trans. Electron Devices* **19** 652
[7] Maloney T J and Frey J 1977 *J. Appl. Phys.* **48** 781
[8] Shur M S and Eastman L F 1981 *Solid-State Electron.* **24** 11
[9] Tanaka S, Kobayashi H, Satito H and Shionoya H 1980 *J. Phys. Soc. Japan* **49** 1051
[10] Graudszus W and Goebel E O 1981 *J. Physique Coll.* **C7** 437
[11] Rosen D, Donkas A G, Bundanky Y, Katy A and Alfano R R 1981 *Appl. Phys. Lett.* **39** 935
[12] Sha W, Norris T B, Schaff W J and Meyer K E 1991 *Phys. Rev. Lett.* **67** 2553
[13] Shank C V, Fork R L, Greene B I, Reinhard F K and Logan R A 1981 *Appl. Phys. Lett.* **38** 104
[14] Meyer K E, Pessot M, Mourou G A, Grondin R O and Chamoun S N 1988 *Appl. Phys. Lett.* **53** 2254
[15] Son J, Sha W, Kim J, Norris T B, Whitaker J F and Mourou G A 1993 *Appl. Phys. Lett.* **63** 923
[16] Hu B B, de Souza E A, Knox W H, Cunningham J E, Nuss M C, Kuznetsov A V and Chuang S L 1995 *Phys. Rev. Lett.* **74** 1689
[17] Mooradian A 1969 *Light Scattering Spectra of Solids* ed G Wright (New York: Springer) p 285
[18] Wolff P A 1969 *Light Scattering Spectra of Solids* ed G Wright (New York: Springer) p 273
[19] Hamilton D C and McWhorter A L 1969 *Light Scattering Spectra of Solids* ed G Wright (New York: Springer) p 309
[20] Jha S S, Kash J A and Tsang J C 1986 *Phys. Rev.* B **34** 5498
Vengurlekar A S and Jha S S 1988 *Phys. Rev.* B **38** 2044
[21] Chia C, Sankey O F and Tsen K T 1992 *Phys. Rev.* B **45** 6509
[22] Chia C, Sankey O F and Tsen K T 1992 *J. Appl. Phys.* **72** 4325
[23] Chia C, Sankey O F and Tsen K T 1993 *Mod. Phys. Lett.* **7** 331
[24] Mooradian A and McWhorter A L 1970 *Proc. 10th Int. Conf. on the Phys. of Semiconductors* ed S P Keller, J C Hansel and F Stern (Oak Ridge, TN: US Atomic Energy Commission) p 380
[25] Ralph S E and Wolga G J 1990 *Phys. Rev.* B **42** 11353
[26] Grann E D, Sheih S J, Chia C, Tsen K T, Sankey O F, Guncer S E, Ferry D K, Maracas G, Droopad R, Salvador A, Botcharev A and Morkoc H 1994 *Appl. Phys. Lett.* **64** 1230
[27] Grann E D, Tsen K T, Sankey O F, Ferry D K, Salvador A, Botcharev A and Morkoc H 1995 *Appl. Phys. Lett.* **67** 1760
[28] Grann E D, Sheih S J, Tsen K T, Sankey O F, Guncer S E, Ferry D K, Salvador A, Botcharev A and Morkoc H 1995 *Phys. Rev.* B **51** 1631
[29] Grann E D, Tsen K T, Ferry D K, Salvador A, Botcharev A and Morkoc H 1996 *Phys. Rev.* B **53** 9838
[30] Grann E D, Tsen K T, Ferry D K, Salvador A, Botcharev A and Morkoc H 1997 *Phys. Rev.* B **56** 9539
[31] Tsen K T, Joshi R P, Salvador A, Botcharev A and Morkoc H 1997 *J. Appl. Phys.* **81** 406

[32] Ferry D K 1991 *Semiconductors* (New York: MacMillan) chapter 13
[33] Ridley B K 1993 *Quantum Processes in Semiconductors* 3rd edn (London: Oxford Press)
[34] Ruf T and Cardona M 1990 *Phys. Rev.* B **41** 10747 and references therein
[35] Varga B B 1965 *Phys. Rev.* A **137** 1896
[36] Kim M E, Das A and Senturia S D 1978 *Phys. Rev.* B **18** 6890
[37] Lugli P and Ferry D K 1985 *Appl. Phys. Lett.* **46** 594